October 2003 • NREL/CP-500-35077

Conference Paper

New Developments for the NWTC's FAST Aeroelastic HAWT Simulator

Preprint

J.M. Jonkman and M.L. Buhl, Jr.

To be presented at the 42nd Aerospace Sciences Meeting and Exhibit Conference
Reno, Nevada
January 5-9, 2004

National Renewable Energy Laboratory

1617 Cole Boulevard
Golden, Colorado 80401-3393

NREL is a U.S. Department of Energy Laboratory
Operated by Midwest Research Institute • Battelle • Bechtel

Contract No. DE-AC36-99-GO10337

NEW DEVELOPMENTS FOR THE NWTC'S FAST AEROELASTIC HAWT SIMULATOR*

Jason M. Jonkman† and Marshall L. Buhl Jr.‡
National Renewable Energy Laboratory (NREL)
National Wind Technology Center (NWTC)
1617 Cole Boulevard
Golden, Colorado 80401-3393 (USA)

ABSTRACT

Discrepancies in response predictions among FAST, ADAMS, and other industry-accepted wind turbine analysis codes led the National Renewable Energy Laboratory to dedicate significant time and effort to overhauling its FAST aeroelastic horizontal-axis wind turbine simulator. Included in the overhaul were improvements to the system dynamics models and upgrades in functionality. Improvements were made to the drivetrain dynamics models, output processing algorithms, tower and blade deflection characterizations, and other models. New features include an enhanced input/output environment, aeroacoustic noise prediction algorithms, periodic linearization routines for controls design, as well as a preprocessing utility that enables FAST to generate ADAMS datasets of wind turbine models. In order to verify that the new features and improved models included in the upgraded FAST were correct, verification tests were run against ADAMS. Comparisons of response predictions between the codes, in general, show excellent agreement. Regions where the different response predictions do not exactly coalesce are attributable to differences in the modeling techniques. This work has culminated in an upgraded version of FAST, equipped with more functionality, that predicts more accurate wind turbine responses than previous versions.

INTRODUCTION

Over the past decade, the U.S. Department of Energy's (DOE's) National Renewable Energy Laboratory (NREL) has sponsored the development, verification, and validation of comprehensive aeroelastic simulators capable of predicting both the extreme and fatigue loads of horizontal-axis wind turbines (HAWTs). These simulation tools, also known as design codes, are used by industry, academia, and government entities for wind turbine design, certification, and research.

In general, these design codes enable a user to (1) define an aerodynamic and structural model of a wind turbine given the turbine geometry and aerodynamic and mechanical properties of its members, and (2) simulate the wind turbine's aerodynamic and structural response by imposing complex, virtual, wind-inflow conditions. Outputs of the simulations include time-series data on the aerodynamic loads, as well as loads and deflections of the structural members of the wind turbine. Post-processing codes are then used to analyze these data.

FAST (Fatigue, Aerodynamics, Structures, and Turbulence) [1] and ADAMS® (Automatic Dynamic Analysis of Mechanical Systems) [2], [3] are two of the most sophisticated design codes used by the U.S. wind industry and the two most promoted by NREL's National Wind Technology Center (NWTC). ADAMS is a commercially available, general purpose, multibody-dynamics code from MSC.Software Corporation that is adaptable for modeling wind turbines. FAST is a structural-response, HAWT-specific code originally developed by Oregon State University and the University of Utah for the NWTC. Both FAST and ADAMS use the University of Utah's AeroDyn aerodynamic subroutine package for calculating aerodynamic forces [4].

Previous comparisons among FAST (previously known as FAST_AD, FAST2, and FAST3 in some literature), ADAMS, and other industry-accepted wind turbine analysis codes have shown reasonable agreement between FAST and ADAMS response predictions [5], [6], [7]. However, after more in-depth evaluations, discrepancies surfaced. Discrepancies showed up in the dynamic responses of more flexible machines and/or systems tested under more taxing conditions and in output channels that were previously untested. A particularly detailed listing of FAST's problems is provided in the author's Master of Science thesis [8]. Additionally, a survey of design-load analysis requirements led to the conclusion that FAST lacked many analysis features, including the capability to model many different types of fault scenarios. These analysis requirements are specified, for example, by the International Electrotechnical Commission (IEC)

†E-mail: jason_jonkman@nrel.gov
‡E-mail: marshall_buhl@nrel.gov

61400-1 standard [9] that governs the safety of utility-scale wind turbines or the IEC 61400-2 standard [10] that governs the safety of small wind turbines.

To address these issues and others, in 2002 the NWTC decided to dedicate significant time and effort in-house to overhaul FAST. The equations of motion (EoMs) and output channel processing algorithms were redeveloped and recoded in the upgraded FAST code to eliminate errors and to improve code maintainability. At the same time, new analysis features were added to FAST so that FAST can be used to model a variety of start-up and shut-down sequences and control events, as well as many common fault scenarios. The new code also includes an enhanced input/output (I/O) environment with coordinate systems and notation corresponding to the IEC 61400-13 standard [11]. In 2003, additional features were added, including the ability to develop periodic linearized state matrices for controls design and the ability to use FAST as a preprocessor for generating ADAMS datasets of wind turbine models.

This paper documents many of the important improvements and new features of FAST and highlights the NWTC's plans for future development of the code. Response predictions that compare FAST with ADAMS are also provided for verification of some of the new conditions that can now be modeled.

NEEDS JUSTIFICATION

Revamping FAST may appear to be a low priority, given the availability of other wind turbine analysis codes such as *BLADED* [12] and general-purpose codes such as ADAMS. However, the development and distribution of improved codes are avenues used by the NWTC to disseminate improved models and technological concepts to the wind community. In many respects, design codes bridge the gap between theorized predictions and experimental and/or observable measurement. Design codes enable virtual experiments capable of yielding load analysis results quickly and cheaply, and in many situations, virtual experimentation offers the only practical method of research and testing. Without continuous investment in the improvement and enhancement of codes such as FAST, the accuracy of this virtual experimentation will not increase. Additionally, the U.S. wind industry has asked for support and improvements to existing codes such as FAST.

FAST also has advantages over many other wind turbine analysis codes, not the least of which is the fact that FAST is *free*. The combination of current analysis features and those proposed establishes FAST as a comprehensive HAWT analysis tool. Moreover, the NWTC has enlisted a staff dedicated to improving FAST as well as other analysis tools it has supported and developed. Germanischer Lloyd (GL), under contract with the NWTC, is also in the process of testing FAST for its acceptance for generating design loads needed for certification to provide additional confidence in its fidelity.

OVERVIEW OF FAST

Before diving into the details of FAST's improvements and upgrades, it is constructive to step back and outline the general class of modeling techniques employed in FAST. For a more detailed description of these methodologies, see the FAST User's Guide [1].

FAST models the blades and tower as individual flexible elements using a modal representation. The flexibility characteristics of these members are determined by specifying distributed stiffness and mass properties along the span of the members and by prescribing their mode shapes through equivalent polynomial coefficients. Torsional flexibility in the drivetrain is modeled using an equivalent linear spring and damper model in the low-speed shaft (LSS). The nacelle and hub are modeled in FAST as rigid bodies with appropriate mass and inertia terms. Time marching of the EoMs is performed using a constant-time-step, Adams-Bashforth-Adams-Moulton, predictor-corrector integration scheme. FAST has a limited number of degrees of freedom (DOFs) but can model most common wind turbine configurations and control scenarios. The DOFs available in FAST can be enabled or disabled through switches, permitting the user to easily increase or decrease the fidelity of the model.

Both FAST and ADAMS use the AeroDyn aerodynamic subroutine package for computing aerodynamic forces [4]. This aerodynamic package models wind turbine aerodynamics using the classic, equilibrium-based, blade-element/momentum (BEM) theory or by using a generalized dynamic inflow model, both of which include the effects of axial and tangential induction. The BEM model uses tip and hub losses as characterized by Prandtl. Dynamic-stall behavior can be characterized using the optional Beddoes-Leishman dynamic stall model.

IMPROVED DYNAMICS MODELING

The EoMs in FAST are derived and implemented using Kane's dynamics. By a direct result of Newton's laws of motion, Kane's EoMs for a simple holonomic system with P generalized coordinates (DOFs) can be stated as follows [13]:

$$F_r + F_r^* = 0 \quad (r = 1, 2, \ldots, P) \tag{1}$$

where for a set of w rigid bodies characterized by reference frame N_i and center of mass point X_i, the generalized active forces are:

$$F_r = \sum_{i=1}^{w} {}^E\boldsymbol{v}_r^{X_i} \cdot \boldsymbol{F}^{X_i} + {}^E\boldsymbol{\omega}_r^{N_i} \cdot \boldsymbol{M}^{N_i} \quad (r = 1, 2, \ldots, P) \tag{2}$$

and the generalized inertia forces are:

$$F_r^* = \sum_{i=1}^{w} {}^E\boldsymbol{v}_r^{X_i} \cdot \left(-m_i \, {}^E\boldsymbol{a}^{X_i}\right) + {}^E\boldsymbol{\omega}_r^{N_i} \cdot \left(-{}^E\dot{\boldsymbol{H}}^{N_i}\right) \quad (r = 1, 2, \ldots, P). \tag{3}$$

In these equations, it is assumed that for each rigid body N_i, the active forces $\boldsymbol{F}^{X_i}$ and $\boldsymbol{M}^{N_i}$ are applied at the center of mass point X_i. The acceleration of the center of mass point X_i is given by ${}^E\boldsymbol{a}^{X_i}$, and the time derivative of the angular momentum of rigid body N_i about X_i in the inertial frame E is given by ${}^E\dot{\boldsymbol{H}}^{N_i}$. The quantities ${}^E\boldsymbol{v}_r^{X_i}$ and ${}^E\boldsymbol{\omega}_r^{N_i}$ represent the partial linear and partial angular velocities, respectively.

Since Kane's equations are composed of vector quantities [reference Eq. (2) and Eq. (3)], the equations can be expressed in terms of reaction loads (which are also vectors) at points within the system. For instance, consider a system with two bodies, A and B. To write the EoMs of body A in terms of the reaction loads between bodies A and B, hypothetically remove body B from the system and determine which "equivalent" loads applied on A produce the same EoMs for body A in the system containing both bodies A and B. These "equivalent" loads applied on body A are the reaction loads between bodies A and B.

This is how the EoMs are implemented in the new version of FAST. The loads from which the EoMs are derived are the same loads available as output. Writing the EoMs in terms of these loads is beneficial since the EoMs solution and determination of output loads is executed in a single step. This is in contrast to earlier versions of FAST that implemented a less elegant and more difficult to maintain two-step approach in which the EoMs were solved first and the output loads were computed second.

Not only is the solution process more elegant, but also the important errors in the original dynamics models of FAST have been eliminated.

One serious modeling error that is fixed in the latest version of FAST relates to the blade structural pretwist. In previous versions of the code, the blade structural pretwist distribution was implemented using the opposite sign convention identified by the user's guide. This inevitably led users to input the blade structural pretwist properties backward. For turbines with stiff blades, the repercussions were minor. For more flexible blades, the dynamic responses were mysteriously inaccurate.

Earlier versions of the code assumed that the orientations of the local blade element coordinate systems, which are used for applying aerodynamic loads to the blade elements, did not change as the blade deflected. This resulted in errors in the application of aerodynamics loads to flexible blades. In the latest version of FAST, the blade element coordinate systems now follow and orient themselves with the deflected blade. This provides a more realistic means of interfacing aerodynamic loads with the blades. The new FAST also supports variably-spaced analysis nodes, allowing the user to focus better resolution of aerodynamic loads in critical regions of the blade. Aerodynamic pitching-moment terms are also included. This latter improvement may be of minor importance, however, since blade torsional DOFs are still absent from the model.

In real life, lateral deflections of the tower have an associated vertical displacement. This dynamic "shortening" effect is now modeled in FAST. In order to illustrate the tower shortening behavior, consider the geometry of a deflected tower that is cantilevered to the ground as shown in Figure 1. h represents the elevation along the flexible portion of a tower of height H. The lateral deflection is u, and the associated vertical displacement is w. The deflection is illustrated at some time t.

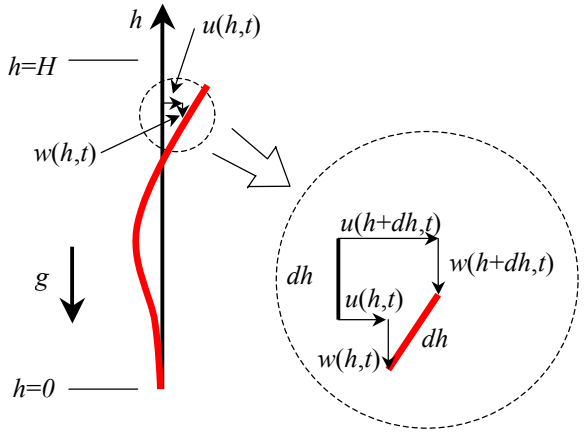

Figure 1: Tower Deflection Geometry at Time *t*

The deflections u and w at elevation $h+dh$ can be expanded using a first order Taylor series approximation. Using these expressions, the Pythagorean theorem can be applied to the geometry of

a deflected tower element (reference the dashed circle magnification of Figure 1) to obtain the following differential relationship:

$$\frac{\partial w(h,t)}{\partial h} = \frac{1}{2}\left[\frac{\partial u(h,t)}{\partial h}\right]^2. \qquad (4)$$

Equation (4) can be integrated over h (using the dummy variable h') to obtain the tower's shortening as a function of the tower's lateral deflection. Since the slope of the tower must be zero at the cantilevered end, the tower shortening becomes:

$$w(h,t) = \frac{1}{2}\int_0^h \left[\frac{\partial u(h',t)}{\partial h'}\right]^2 dh'. \qquad (5)$$

Equation (5) is the relationship governing the dynamic shortening of the tower as implemented in the new version of FAST. The tower's vertical displacement, velocity, and acceleration are all affected by the shortening effect. This dynamic shortening effect is also included in the blade models. Inclusion of the shortening effects improves the dynamic modeling of the complete system and permits better correlation of the rotor to the wind inflow.

The drivetrain dynamics models have also been improved. Two of the most important are improvements to the high-speed shaft (HSS) brake and yawing-induced gyroscopic pitching moment models.

The new HSS brake model is based on the Coulomb model of sliding friction. The braking torque as a function of shaft speed is depicted in Figure 2. The magnitude of the brake torque is constant as long as the shaft speed is nonzero. When the speed is zero, the torque takes on any value between its constant limits to prevent motion of the shaft (the shaft can move only if external torques exceed the braking torque limits).

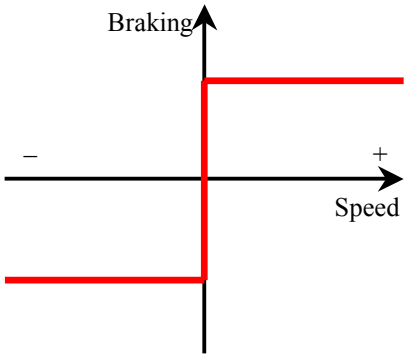

Figure 2: Braking Torque-Shaft Speed Relationship

It is numerically difficult to model this torque-speed relationship within the vertical region of the curve. Consider the case in which the brake is applied and the rotor is decelerating. As time progresses, the shaft speed moves leftward in Figure 2. Since FAST operates in discrete time, the shaft speed will decrement in finite-size steps every time increment. As the speed approaches the vertical region of the curve, it is possible that the step in speed will pass over the vertical region within a time increment, causing the shaft speed to change directions. This is a physically impossible situation since the brake will grab hold and "lock" the shaft once the speed reaches zero.

To prevent the shaft from passing through the vertical region, FAST now calculates the braking torque necessary to bring the shaft speed to zero at each time increment (this technique is similar to the Lagrange multiplier method of finding constraint reactions). The value of this braking torque is used as long as it does not exceed the limits of the brake. This technique ensures that the brake locks the shaft during a shutdown maneuver, bringing about realistic dynamic loads and "ringing" behavior. Older versions of FAST replaced the vertical region of the curve with a parabolic ramp. This eliminated the numerical difficulties, but it also eliminated the ringing behavior brought about by locking of the shaft by the brake.

Gyroscopic pitching moments are induced when the nacelle yaws while the drivetrain is spinning. These moments and resulting dynamic responses can be significant if either the angular momentum of the drivetrain or the yawing precession rate is large. When a generator with rotational inertia J rotates at rate $\boldsymbol{\omega}$, the pitching moment induced gyroscopically by the generator, $\boldsymbol{M}$, is as follows:

$$\boldsymbol{M} = \boldsymbol{\Omega} \times (J\boldsymbol{\omega}) \qquad (6)$$

where $\boldsymbol{\Omega}$ is the precession rate associated with yawing. The term in parentheses represents the angular momentum of the drivetrain. The pitching moment, $\boldsymbol{M}$, is orthogonal to both $\boldsymbol{\omega}$ and $\boldsymbol{\Omega}$. It is important to note that the rotor also produces a gyroscopic pitching moment. However, even though a rotor's inertia is much larger than a generator's inertia, the angular momentum of a generator can be of the same order of magnitude as that of a rotor, since the generator is generally spinning much faster than the rotor.

Upon careful inspection of Eq. (6), it is seen that the resulting pitching moment depends on whether the HSS is lumped to the LSS in the model. This is because the magnitudes of J and $\boldsymbol{\omega}$ depend on how the HSS is modeled. When the HSS is not lumped to the LSS, J is

the physical inertia of the generator and ω is the HSS speed, equal to the product of the LSS speed and the gearbox ratio. Thus, the pitching moment is linearly proportional to the gearbox ratio. When the HSS is lumped to the LSS, ω is the LSS speed and J is the inertia of the generator cast to the LSS, found by multiplying the physical inertia with the gearbox ratio squared. Thus, the pitching moment is proportional to the square of gearbox ratio and different from when the HSS is not lumped to the LSS side of the gearbox. In the new version of FAST, the former, more realistic HSS model is incorporated, resulting in more accurate gyroscopically induced pitching moments and ensuing dynamic responses.

The improved dynamics models also include the offset between the tower-top and the shaft axis, different mode shapes in each tower direction, and a nacelle tilt DOF, whereas earlier versions of the FAST code did not include these features. Many additional errors and bugs in the dynamics model and output processing have also been eliminated.

NEW FUNCTIONALITY

Modern HAWTs try to improve performance and reduce loads by actively controlling many aspects of the turbine operation. With this in mind, the NWTC added many new control schemes to FAST. Setting certain parameters in the input file enables many common types of control. Users can also implement far more sophisticated controls by supplying their own control routines that can easily be linked to the rest of FAST.

One of the most common forms of turbine control is full-span blade pitch control. Independent or collective rotor blade pitch control is now possible using simple time-based maneuvers (pitch ramps) or by interfacing sophisticated, user-defined control schemes. These schemes can be used, for example, to control power in Region 2 (below rated wind speed) or rotor speed in Region 3 (above rated wind speed). Handles now built into FAST make interfacing user-defined routines an easy task. The simple pitch ramp control inputs enable the user to model many common fault scenarios or override pitch maneuvers.

Two new torque-speed models have been added to FAST. The first is a simple variable-speed control feature in which the electrical generator torque is proportional to speed squared in Region 2 and then constant in Region 3 operation. The second is a generator model that implements the Thevenin-Equivalent-Circuit equations for a three-phase induction generator. This model can be used to more accurately model start-up, shut-down, and overspeed situations. Moreover, the generators can now be switched on and off to simulate connection and disconnection to the electrical grid.

In order to support the modeling of additional shut-down techniques, the tip brakes in FAST can now be deployed at specified times or rotor speeds. This can be done for each blade independently. The HSS brake can also be turned on and off.

A series of semi-empirical aeroacoustic noise prediction algorithms have also been incorporated into FAST. The algorithms predict six forms of aerodynamically produced noise, including turbulent inflow, turbulent boundary layer trailing edge, separating flow, laminar boundary layer vortex shedding, trailing edge bluntness vortex shedding, and tip vortex formation. These noise sources are then superimposed to calculate and output the total aeroacoustic signature of an operating wind turbine. Details on the contents and validation of these aeroacoustic noise prediction models are provided in [14].

Additional outputs are also available for time-marching analyses. All six components of loads (three forces and three moments) are now available at most critical locations within the system, as are the displacements, velocities, and accelerations (both linear and angular) of critical bodies within the system.

Linearization

To aid in controls design and analysis, linearization routines have also been added to FAST. This analysis feature can also be used to determine full system modes of an operating or stationary HAWT by using a simple eigenanalysis. The linearization routines follow a procedure similar to that used by the Symbolic Dynamics (SymDyn) code, which is a controls-oriented HAWT analysis tool also developed by researchers at the NWTC [15].

The linearization process consists of two steps: (1) computing a periodic steady state operating point condition for the DOFs, and (2) numerically linearizing FAST about this operating point to form periodic state matrices. The output state matrices can be azimuth-averaged for nonperiodic, or time-invariant, controls development.

In the first step, for variable-speed machines, FAST can trim either electrical generator torque (for Region 2 control) or rotor collective blade pitch (for Region 3 control) while maintaining the other control input constant in order to reach a desired azimuth-averaged rotor speed. For constant-speed machines, the trim analysis is bypassed when computing the periodic

operating point. User-specified initial conditions can also be chosen as the operating point.

Once a periodic operating point has been found, FAST numerically linearizes the EoMs to find state matrices at each azimuth step of the periodic solution. The linearization routines can be used to develop a first or second order representation of the EoMs. The EoMs per Eq. (1) can be written in matrix form as follows:

$$M\left(\underline{q},\underline{u},t,\right)\underline{\ddot{q}}+\underline{f}\left(\underline{q},\underline{\dot{q}},\underline{u},\underline{u}_d,t\right)=\underline{0} \tag{7}$$

where M is the mass matrix, $\underline{f}$ is the nonlinear forcing function, $\underline{q}$ is the vector of DOF states (and $\underline{\dot{q}}$ and $\underline{\ddot{q}}$ are the first and second state derivates), $\underline{u}$ is the vector of control inputs, $\underline{u}_d$ is the vector of wind inputs, and t is time. The second order representation of these equations, as output by FAST is:

$$M\,\underline{\Delta\ddot{q}}+C\,\underline{\Delta\dot{q}}+K\,\underline{\Delta q}=F\,\underline{\Delta u}+F_d\,\underline{\Delta u}_d \tag{8}$$

where M, C, and K are the mass, damping, and stiffness matrices, respectively. F is the input matrix, and F_d is the input disturbance matrix. The Δ-symbol is used to indicate perturbations of the states, control inputs, and wind inputs (i.e., input disturbances) about their periodic operating point conditions.

The vectors $\underline{\Delta q}$, $\underline{\Delta\dot{q}}$, and $\underline{\Delta\ddot{q}}$ are replaced with the first order state vectors, $\underline{x}$ and $\underline{\dot{x}}$:

$$\underline{x}=\begin{Bmatrix}\underline{\Delta q}\\ \underline{\Delta\dot{q}}\end{Bmatrix} \text{ and } \underline{\dot{x}}=\begin{Bmatrix}\underline{\Delta\dot{q}}\\ \underline{\Delta\ddot{q}}\end{Bmatrix} \tag{9}$$

to determine the first order representation of the EoMs:

$$\underline{\dot{x}}=A\underline{x}+B\underline{\Delta u}+B_d\underline{\Delta u}_d\,. \tag{10}$$

In this form, the state matrix A, input matrix B, and input disturbance matrix B_d are related to their second order counterparts as follows:

$$A=\begin{bmatrix}0 & I\\ -M^{-1}K & -M^{-1}C\end{bmatrix},\ B=\begin{bmatrix}0\\ M^{-1}F\end{bmatrix}, \text{ and } B_d=\begin{bmatrix}0\\ M^{-1}F_d\end{bmatrix} \tag{11}$$

where I is the identity matrix.

Along with the linearized EoMs, FAST also develops the linearized system associated with output measurements $\underline{y}$, which for a first order representation is as follows:

$$\underline{y}=C\underline{x}+D\underline{\Delta u}+D_d\underline{\Delta u}_d\,. \tag{12}$$

Matrices C, D, and D_d are the output state, transmission, and disturbance transmission matrices, respectively.

ADAMS Preprocessor

The upgraded version of FAST also has the capability of extracting "equivalent" ADAMS wind turbine datasets from the turbine properties specified in the FAST input files(s). That is, FAST has the functionality of acting like an ADAMS-preprocessor capable of creating ADAMS datasets of wind turbine models through FAST's simple property-input-style interface. Thus, FAST can be used as an alternative to the ADAMS/WT toolkit or other preprocessors used to create ADAMS datasets of wind turbine models.

The ADAMS datasets extracted from FAST contain all the functionality and usability associated with the FAST model while bypassing some of FAST's limitations. The extracted ADAMS datasets have a few minor limitations, which will be highlighted later.

All the turbine control paradigms available in FAST are incorporated into the ADAMS model. These include the functionality of pitching the blades, controlling the generator torque, applying the HSS brake, and deploying the tip brakes. The ADAMS datasets incorporate the same generator, drivetrain, yaw, tilt, teeter models, and DOFs used by FAST. Also, all of the output parameters specified at the end of FAST's primary input file are passed into the ADAMS datasets. This eliminates the need to develop a REQSUB() user-written subroutine for request output every time an ADAMS dataset is generated. Once an ADAMS analysis is run, the format of ADAMS' output file containing time-series data is identical to that of FAST's so that post-processing techniques are compatible for the codes.

One of FAST's limitations that ADAMS bypasses is the assumed-mode approximation of the blades and tower. The blades and tower of the extracted ADAMS model are developed from FAST's distributed mass and stiffness inputs using ADAMS' conventional approach of modeling flexible members through a series of lumped masses connected by stiffness and damping FIELDs. Nevertheless, FAST's valuable DOF-switching functionality is still available in the ADAMS model, so these flexibilities can be eliminated through a simple switch, just as they can be in FAST (in ADAMS the flexibilities are eliminated collectively, not one mode at a time).

Moreover, several characteristics not implemented in the FAST model are incorporated into the extracted ADAMS model. These include torsional and

extensional DOFs for the blades and tower, mass and elastic offsets for the blades, mass offsets for the tower, actuator dynamics for the blade pitch controls, and graphical output capabilities.

FAST CERTIFICATION PROCEDURE

Whenever we produce a new version of FAST, we execute an automated procedure that runs a series of simulations using different turbine models that operate with various features enabled under a variety of wind conditions. This automated certification procedure is useful for determining whether we have fixed a problem or to insure that we have not created any new problems when altering FAST. For each test, we generate about two dozen output parameters, which vary from test to test. Of the roughly 200 unique output parameters available in FAST, we output nearly 85% of them in at least one test and about 65% of them in at least two tests.

Depending on the type of simulation, we examine the data in different ways. In addition to basic statistics, we sometimes generate azimuth averages or probability-mass functions, which show the probability that a given parameter will fall within a range of values.

COMPARISONS TO ADAMS

For our comparisons to ADAMS we used FAST v4.31, AeroDyn v12.56, and ADAMS 12.0. We generated our ADAMS datasets using the FAST-to-ADAMS preprocessing capability of FAST. We used SNwind v1.20 [16] to generate full-field turbulent wind files for some of the test cases, and we computed statistics, azimuth averages, and probability-mass functions (PMFs) using Crunch v2.83 [17].

We did not compare simulation predictions to test data for several reasons. First, we do not have all the turbine properties needed to make accurate models that will be worth comparing to test data. Because of this, we often had to invent elements like tower properties. The other reason is that most test data are hard to use. For field tests, it is very difficult to know what the true inflow is, so differences in model predictions can differ from test data because the model properties are incorrect, errors exist in the algorithms or coding, and because the turbine did not actually experience the measured inflow. Wind-tunnel tests are more useful, so we modeled the NWTC's Unsteady Aerodynamics Experiment (UAE) turbine in the NASA Ames wind tunnel for some of our tests. We did not have time to tune our input properties (especially the airfoil data) to the test data for this paper. We hope to do so in the future.

We model four turbines with a variety of configurations for this effort. The turbines were chosen because we can publish the models and freely distribute them with the FAST archives. We modeled the AWT-27CR2, a 27-m, free-yaw, downwind, two-bladed, teetering turbine. We also modeled the AOC 15/50, a 15-m, free-yaw, downwind, three-bladed turbine. Our third turbine is the 10-m UAE Phase VI turbine. This turbine has two blades, can run either upwind or downwind, and has a teeter hinge that can be locked. The fourth turbine is a paper turbine that was designed by Global Energy Concepts and Windward Engineering for the NWTC's WindPACT Rotor Study. It is a typical 1.5-MW, Danish-style turbine. It has three blades, runs upwind, has full-span pitch control, and is variable speed. FAST can model the variable-speed and variable-pitch controls, but it does not currently have the capability to model the yaw control.

Because of space limitations for this paper, we can only show a few comparison plots and discuss a few of the tests. For additional results, all plots are available on our Web server (http://wind.nrel.gov/designcodes/fast/verification/).

Our first test is the AWT-27CR. All appropriate DOFs are enabled except for the yaw DOF. We locked the yaw so that there is a net 15° yaw error. We computed azimuth averages of 23 output parameters and plotted the results. The plot of teeter deflection (not given here) shows that FAST and ADAMS agree so well that the ADAMS curve cannot be distinguished from the FAST curve. For this test, many of the plots showed nearly perfect agreement, but some, such as tower-top displacements, velocities, and accelerations, show a difference of 5%-10%. Figure 3 shows a plot of the root bending moments for Blade 1. As you can see, the agreement for this parameter is excellent.

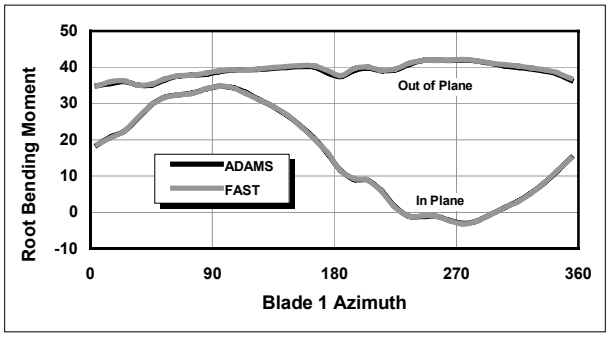

Figure 3: Azimuth Averages of Blade Root Bending Moments for the AWT-27CR2

The second test also used our AWT-27CR2 model. It comprised a motor start-up (t=6) followed by a loss of grid (t=12) and then deployment of the HSS brake (t=13). We used the Thevenin-Equivalent Circuit model for the generator. All 22 output parameters show virtually identical predictions for the two codes. For instance, Figure 4 shows a plot of the rotor speed.

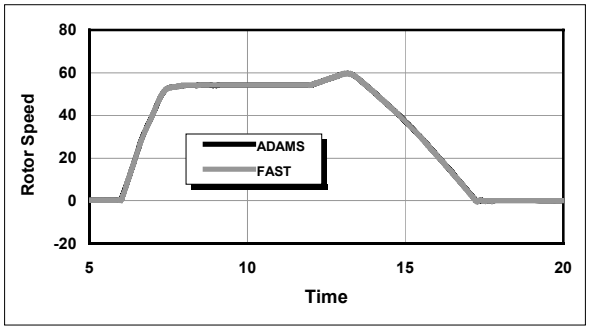

Figure 4: Rotor-Speed Response for a Start-Up, Loss of Grid, and Shut-Down Using a HSS Brake for the AWT-27CR2 Turbine

Test 3 is similar to Test 1, except we allowed the turbine to yaw freely and we also changed a few of the AeroDyn options. In previous comparisons between FAST_AD and ADAMS [7], we did not test models with free-yaw because the equilibrium yaw positions were different enough to mask all other results. With the improvements made to FAST over the past two years, this is no longer an issue, as can be seen in Figure 5.

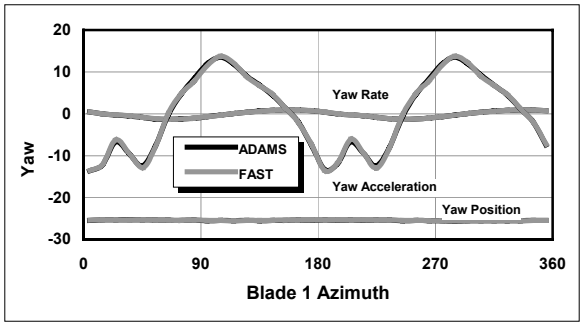

Figure 5: Yaw Response for the AWT-27CR2 Turbine to a Steady 12 m/s Wind at 30°

Test 4 also used the AWT-27CR2 model, but we drove it with full-field turbulence generated by SNwind. We generated PMFs to compare the results. All but two of the 18 tested parameters show excellent agreement. The first is a plot of the flap bending moment at the 86% station (see Figure 6), which is the second to last station from the tip. The loads predicted by FAST are generally higher than those predicted by ADAMS. This is caused by the fundamental difference in the way the two codes model the blade structure. FAST divides the blade into segments and distributes mass across the expanse of each segment. ADAMS lumps all of its mass at the center of each segment (rigid body inertia effects are also included). FAST includes the mass in the blade segment outboard of the center of the segment when calculating the load at the center of the segment. ADAMS, with its lumped-inertia approach, is less accurate. This difference shows most in the outboard part of the blade and becomes insignificant toward the root.

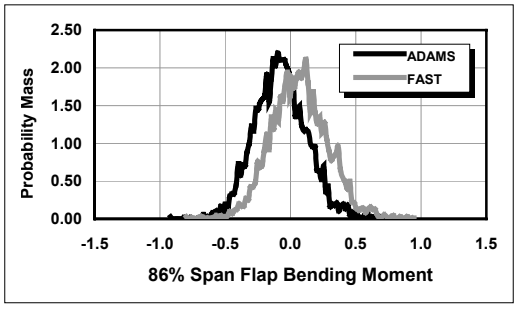

Figure 6: PMF of the 86% Span Flap Bending Moment of the AWT-27CR2 Turbine Operating in Free Yaw with Full-Field Turbulence

The second chart from Test 4 depicts the tower-top pitching moment. As can be seen in Figure 7, ADAMS predicts a much wider spread in moments. This is caused by a fundamental limitation in ADAMS that manifests itself when modeling a rapidly yawing turbine (most common with free-yaw turbines) that has a gearbox. ADAMS has numerical difficulties modeling elements, like generator rotors, that rotate at high speeds, such as 1800 rpm. In such cases, the solution is at best very inefficient and at worst inaccurate. To avoid this problem and still be able to model the rotational inertia effects of the generator rotor on the drivetrain dynamics, the HSS should be lumped to the LSS as described in the "Improved Dynamics Modeling" section of this paper. This ensures that the generator will rotate at LSS speeds instead of HSS speeds. The effects of this modeling approach are shown in Figure 7. Since FAST models the HSS properly, this is one situation in which FAST is superior to ADAMS.

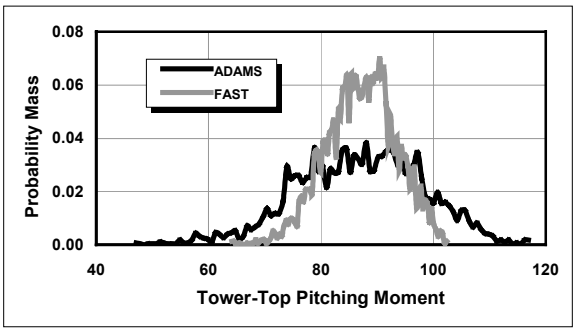

Figure 7: Probability Mass Function of the Tower-Top Pitching Moment of the AWT-27CR2 Turbine Operating in Free Yaw with Full-Field Turbulence

Test 5 is similar to Test 2, but we configured the tip brakes to self-deploy at a given overspeed rotor condition instead of using the HSS brake. As in Test 2, agreement between FAST and ADAMS is excellent.

Tests 6 through 8 use our AOC 15/50 model. Test 6 exhibits a generator start-up, loss of grid, and tip brake shutdown; Test 7 tests free yaw; and Test 8 features a fixed yaw error. The trends are very similar to the results of Tests 1 through 5, so we won't show the response comparisons here.

Tests 9 and 10 use our UAE Phase VI turbine model. We allowed the turbine to freely yaw in Test 9. One feature available in ADAMS that is not available in FAST is the ability to set the blade-segment center of masses away from the pitch axis. We used that in our ADAMS model for Test 9, and you can see the effect in the plot of blade root edge bending in Figure 8.

Figure 8: Blade Root Edge Bending for the UAE Phase VI Turbine

For Test 10, we modeled the UAE turbine with no DOFs while ramping up the wind speed to predict a power curve. We instructed AeroDyn to generate aerodynamic data for the blade elements. Plots of angle of attack and induction factors show that the predictions from ADAMS and FAST are indistinguishable, so we will not show them here.

Test 11 modeled the WindPACT 1.5-MW turbine exhibiting a pitch failure of one blade. While the turbine was operating with normal pitch control, we caused Blade 1 to change its pitch from the control-system-commanded pitch angle (~11°) at 13 seconds and ramp it to 45° over the next 2 seconds. Figure 9 shows what happens to the out-of-plane tip deflections of Blades 1 and 3. Except for an unexplained difference in Blade 3 at around 15 seconds, ADAMS and FAST agree extremely well. This test and others not documented here demonstrate that FAST's modal approach to modeling blades is acceptable for flexible blades and taxing conditions.

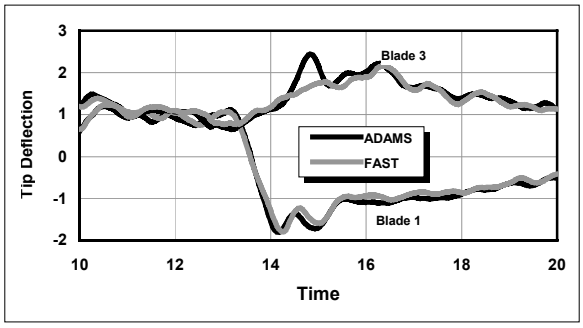

Figure 9: Out-of-Plane Tip Deflections of the WindPACT 1.5-MW Baseline Turbine in Response to a Runaway Pitch of Blade 1

Test 12 also modeled the WindPACT 1.5-MW turbine, this time undergoing an extreme gust with direction change (the IEC ECD case). The ADAMS predictions show generally good agreement with FAST, but they exhibit spikes in some of the parameters. The spikes are caused by the way the ADAMS preprocessor constructs the pitch actuator. FAST sets the blade pitch to the desired pitch commanded by the control system, but ADAMS must supply a torque to the blade's rotational inertia in order to rotate it.

Test 13 modeled the WindPACT 1.5-MW turbine under normal operation. The PMF plots of most of the parameters show excellent agreement, and as such, are not displayed here.

In Test 14 we perform an eigenanalysis on the WindPACT 1.5-MW turbine for verification of FAST's new linearization routines. The eigenanalysis is performed on the stationary turbine (not spinning) and ignores gravitational and aerodynamic loads, as well as structural damping. Results for the first 10 full system

natural frequencies are listed in Figure 10. In FAST, these are obtained by performing an eigenanalysis on the outputted first order state matrix *A* in MATLAB®. In ADAMS, the frequencies are obtained by invoking a "LINEAR/EIGENSOL" command, which linearizes the complete ADAMS model and computes eigendata. Again, the agreement between FAST and ADAMS is quite good.

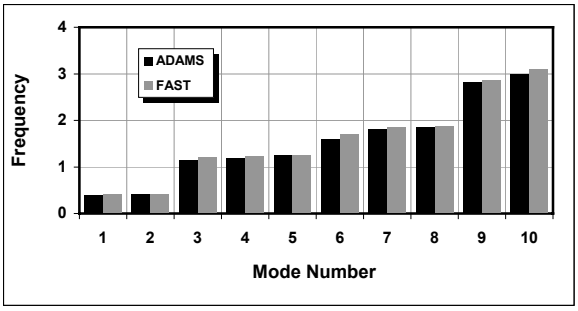

Figure 10: Full System Natural Frequencies of the Stationary WindPACT 1.5-MW Turbine

CONCLUSIONS

The discovery of discrepancies in response predictions among FAST, ADAMS, and other industry-accepted wind turbine analysis codes led the NWTC to dedicate significant time and effort into overhauling FAST. During the overhaul process, FAST's inherent dynamics models were improved to eliminate errors, enhance performance, and improve code maintainability. Improvements were made to the drive-train dynamics models, output processing algorithms, tower and blade deflection characterizations, the interface between the blade structure and AeroDyn, and other models.

At the same time, new analysis features were added to FAST so that FAST can be used to model a variety of start-up and shut-down sequences and control events, as well as many common fault scenarios. The new code also includes an enhanced I/O environment, the ability to develop periodic linearized state matrices for controls design, and a preprocessing utility that enables FAST to generate ADAMS datasets of wind turbine models. Aeroacoustic noise prediction algorithms have also been introduced into FAST.

In order to verify the correctness of the new features and improved models included in the upgraded FAST, verification tests were run against ADAMS. The ADAMS datasets were generated using the FAST-to-ADAMS preprocessing utility. The verification study consisted of test cases in which response predictions from FAST and ADAMS were compared in a side-by-side fashion. In most cases, the agreement between the codes is excellent. Most of the instances in which the code's response predictions do not exactly coalesce are attributable to weaknesses in one of the models. Most of FAST's weaknesses lie in its inability to model mass and elastic offsets in the blades and tower. Most of ADAMS weaknesses lie in its difficulty modeling quickly rotating elements, such as generators.

This work has culminated in an upgraded version of FAST, equipped with more functionality, that predicts more accurate wind turbine responses than previous versions.

FUTURE WORK

The NWTC is planning to incorporate additional DOFs and functionality to FAST in the near future. On the docket are plans to add foundation flexibility models and associated DOFs, earthquake loading, and wave loading dynamics. In order to support small wind turbine research initiatives, functionality associated with furl behavior will also be added to FAST. Furling DOFs under consideration include a furl axis between the yaw system and the nacelle, as well as a hinge between the nacelle and tail. Tail aerodynamics models will also be integrated to the code. Drivetrain shaft bending DOFs will also be added so that users can predict the important dynamics associated with whirl of the shaft.

As more complexity is added to the code, the NWTC is committed to completing additional verification studies. One such study is already in the works as FAST and ADAMS are being tested by GL in partnership with the NWTC.

ACKNOWLEDGMENTS

The authors would like to thank everyone who helped with this work, including Alan Wright of NREL for directing the original effort for FAST and for the many improvements he made to the code; Bob Wilson and Ping Heh of Oregon State University, from which FAST originated; David Laino and Craig Hansen of Windward Engineering, for creating AeroDyn and interfacing it to FAST; the FAST-user community for their invaluable feedback related to code improvement; and Ruth Baranowski of NREL, for making this paper much more readable.

Thanks also go to all the managers at the U.S. DOE and NREL who allowed this work to be done the right way. Special thanks go to Robert Thresher, Brian Smith, Mike Robinson, and Sandy Butterfield, without whom these codes would not be as accurate as they are today.

This work was performed at NREL in support of the U.S. DOE under contract number DE-AC36-99-GO10337.

REFERENCES

[1] Jonkman, J.M.; Buhl Jr., M.L. *FAST User's Guide*, NREL/EL-500-29798. Golden, Colorado: National Renewable Energy Laboratory, 2003.

[2] Laino, D.J.; Hansen, A.C. *User's Guide to the Computer Software Routines AeroDyn Interface for ADAMS®*, Windward Engineering, 2001.

[3] Elliott, A.S. (1989). "Analyzing Rotor Dynamics with a General-Purpose Code," *Mechanical Engineering* 112, no. 12 (December 1990): pp. 21–25.

[4] Laino, D.J.; Hansen, A.C. *User's Guide to the Wind Turbine Aerodynamics Computer Software AeroDyn*, Windward Engineering, 2002.

[5] Buhl Jr., M.L.; Wright, A.D.; Tangler, J.L. "Wind Turbine Design Codes: A Preliminary Comparison of the Aerodynamics." *Prepared for the 17th American Society of Mechanical Engineers (ASME) Wind Energy Symposium*, *January 12 - 15, 1998, Reno, Nevada*. NREL/CP-500-23975. Golden, CO: National Renewable Energy Laboratory, December 1997.

[6] Buhl Jr., M.L.; Wright, A.D.; Pierce, K.G. "Wind Turbine Design Codes: A Comparison of the Structural Response." *Proceedings, 2000 American Society of Mechanical Engineers (ASME) Wind Energy Symposium/38th American Institute of Aeronautics and Astronautics (AIAA) Aerospace Sciences Meeting and Exhibit, Reno, Nevada.* AIAA-2000-0022, January 2000, pp. 12–22.

[7] Buhl Jr., M.L.; Wright, A.D.; Pierce, K.G. "FAST_AD Code Verification: A Comparison to ADAMS." *Proceedings, 2001 American Society of Mechanical Engineers (ASME) Wind Energy Symposium/39th American Institute of Aeronautics and Astronautics (AIAA) Aerospace Sciences Meeting and Exhibit, Reno, Nevada.* AIAA-2000-0062, January 2001, pp. 368–377.

[8] Jonkman, J.M. *Modeling of the UAE Wind Turbine for Refinement of FAST_AD*, M.S. Thesis, Colorado State University: Department of Mechanical Engineering, 2001.

[9] IEC 61400-1 ed. 2, *Wind Turbine Generator Systems – Part 1: Safety Requirements*, International Electrotechnical Commission (IEC), 1999.

[10] IEC 61400-2 ed. 1, *Wind Turbine Generator Systems – Part 2: Safety of Small Wind Turbines*, International Electrotechnical Commission (IEC), 1996.

[11] IEC/TS 61400–13 ed. 1, *Wind Turbine Generator Systems – Part 13: Measurement of Mechanical Loads*, International Electrotechnical Commission (IEC), 2001.

[12] Bossanyi, E.A. *BLADED for Windows Theory Manual*. Bristol, England: Garrad Hassan and Partners Limited, September, 1997.

[13] Kane, T.R.; Levinson, D.A. *Dynamics: Theory and Applications*, McGraw-Hill Inc., New York, 1985.

[14] Moriarty, P.J.; Migliore, P.G. *Semi-Empirical Aeroacoustic Noise Prediction Code for Wind Turbines*, NREL/TP-500-34478. Golden, Colorado: National Renewable Energy Laboratory, 2003.

[15] Stol, K.A.; Bir, G.S. *SymDyn User's Guide*, NREL/EL-500-33845. Golden, Colorado: National Renewable Energy Laboratory, 2003.

[16] Buhl Jr., M.L. *SNwind User's Guide*, NREL/EL-500-30121. Golden, Colorado: National Renewable Energy Laboratory, 2003.

[17] Buhl Jr., M.L. *Crunch User's Guide*, NREL/EL-500-30122. Golden, Colorado: National Renewable Energy Laboratory, 2001.

REPORT DOCUMENTATION PAGE

Form Approved
OMB NO. 0704-0188

1. AGENCY USE ONLY (Leave blank)	2. REPORT DATE	3. REPORT TYPE AND DATES COVERED
	October 2003	Conference Paper

4. TITLE AND SUBTITLE
New Developments for the NWTC's FAST Aeroelastic HAWT Simulator: Preprint

5. FUNDING NUMBERS
WER4 3102

6. AUTHOR(S)
J.M. Jonkman, M.L. Buhl, Jr.

7. PERFORMING ORGANIZATION NAME(S) AND ADDRESS(ES)
National Renewable Energy Laboratory
1617 Cole Blvd.
Golden, CO 80401-3393

8. PERFORMING ORGANIZATION REPORT NUMBER
NREL/CP-500-35077

9. SPONSORING/MONITORING AGENCY NAME(S) AND ADDRESS(ES)

10. SPONSORING/MONITORING AGENCY REPORT NUMBER

11. SUPPLEMENTARY NOTES
NREL Technical Monitor:

12a. DISTRIBUTION/AVAILABILITY STATEMENT
National Technical Information Service
U.S. Department of Commerce
5285 Port Royal Road
Springfield, VA 22161

12b. DISTRIBUTION CODE

13. ABSTRACT *(Maximum 200 words)*
Discrepancies in response predictions among FAST, ADAMS, and other industry-accepted wind turbine analysis codes led the National Renewable Energy Laboratory to dedicate significant time and effort to overhauling its FAST aeroelastic horizontal-axis wind turbine simulator. Included in the overhaul were improvements to the system dynamics models and upgrades in functionality. Improvements were made to the drivetrain dynamics models, output processing algorithms, tower and blade deflection characterizations, and other models. New features include an enhanced input/output environment, aeroacoustic noise prediction algorithms, periodic linearization routines for controls design, as well as a preprocessing utility that enables FAST to generate ADAMS datasets of wind turbine models. In order to verify that the new features and improved models included in the upgraded FAST were correct, verification tests were run against ADAMS. Comparisons of response predictions between the codes, in general, show excellent agreement. Regions where the different response predictions do not exactly coalesce are attributable to differences in the modeling techniques. This work has culminated in an upgraded version of FAST, equipped with more functionality, that predicts more accurate wind turbine responses than previous versions.

14. SUBJECT TERMS
wind energy; wind turbine; horizontal axis wind turbine; FAST; analysis codes; ADAMS

15. NUMBER OF PAGES

16. PRICE CODE

17. SECURITY CLASSIFICATION OF REPORT	18. SECURITY CLASSIFICATION OF THIS PAGE	19. SECURITY CLASSIFICATION OF ABSTRACT	20. LIMITATION OF ABSTRACT
Unclassified	Unclassified	Unclassified	UL